iScience

Article

Ocean warming drives tissue-wide metabolic reprogramming in a fish

Graphical abstract

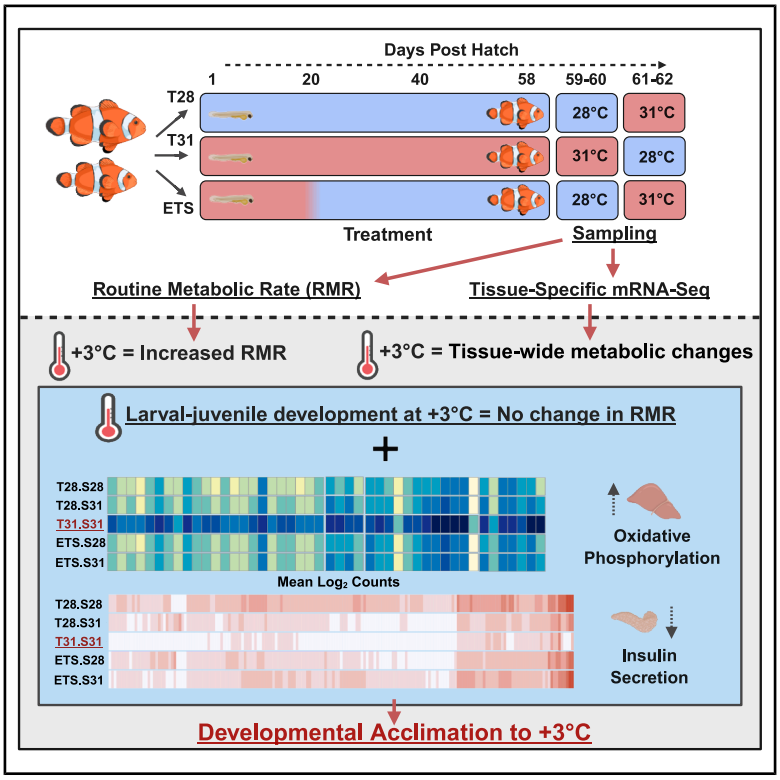

Highlights

- Physiological and molecular response of clownfish to developmental thermal stress
- Developmental warming eliminates the effects of +3°C on clownfish metabolic rates
- Warming induces tissue-wide transcriptomic changes to multiple metabolic processes
- Molecular alterations in the liver-pancreas axis underpin acclimation to warming

Authors

Billy Moore, Shannon McMahon, Michael Izumiyama, Taewoo Ryu, Timothy Ravasi

Correspondence

taewoo.ryu@oist.jp (T.R.), timothy.ravasi@oist.jp (T.R.)

In brief

Zoology; Animal physiology; Molecular physiology

Moore et al., 2025, iScience *28*, 113395
September 19, 2025
https://doi.org/10.1016/j.isci.2025.113395

CellPress

iScience

CellPress
OPEN ACCESS

Article

Ocean warming drives tissue-wide metabolic reprogramming in a fish

Billy Moore,[1,3] Shannon McMahon,[1,2] Michael Izumiyama,[1] Taewoo Ryu,[1,*] and Timothy Ravasi[1,2,*]
[1]Marine Climate Change Unit, Okinawa Institute of Science and Technology Graduate University, 1919-1 Tancha, Onna-son, Okinawa 904-0495, Japan
[2]ARC Centre of Excellence for Coral Reef Studies, James Cook University, Townsville, QLD 4811, Australia
[3]Lead contact
*Correspondence: taewoo.ryu@oist.jp (T.R.), timothy.ravasi@oist.jp (T.R.)
https://doi.org/10.1016/j.isci.2025.113395

SUMMARY

Ocean warming and marine heatwaves are predicted to have adverse impacts on marine organisms. Yet, knowledge of the molecular mechanisms that underpin successful or failed acclimation to increasing temperatures remains incomplete. We conducted an aquaria-based study of early-life stage clownfish comprising of six thermal regimes, measuring the metabolic, and multi-tissue transcriptional response of *Amphiprion ocellaris* using seven tissues. Sampling at 31°C increased metabolic rates in fish reared at 28°C; however, these effects were reduced with increasing developmental rearing at 31°C. Transcriptomic analysis revealed multi-tissue reprogramming of metabolic processes at +3°C, particularly in the liver-pancreas axis. Importantly, chronic larval-juvenile exposure to +3°C induced the acclimation of metabolic rates and caused the upregulation of oxidative phosphorylation (liver) and the downregulation of insulin secretion (pancreas). These results indicate that temperature increase will drive tissue-wide metabolic reprogramming in fish, with changes in key energetic pathways underpinning fish's ability to acclimate to warming.

INTRODUCTION

Owing to sustained anthropogenic CO_2 emissions, mean sea surface temperatures are predicted to increase by up to 4°C by 2100.[1] Additionally, short-term increases in temperature (marine heatwaves; MHWs) are projected to increase in intensity as climate change advances.[2,3] These changes are expected to disrupt marine ecosystems, with coral reefs, kelp forests, seagrass meadows, and their inhabitants amongst the most vulnerable.[4] Of these inhabitants, fish display altered metabolism, growth, reproduction, and behavior at elevated temperatures.[5–8] These physiological impacts are coupled with broader observations of reduced abundance, diversity, and survival, underlining the negative impacts of ocean warming and MHWs on fish.[9–11] Nevertheless, as future ocean warming will encapsulate multiple life-stages of fish, developmental acclimatory processes may alter the currently predicted impacts of ocean warming and MHWs. Such acclimation depends upon developmental programming, defined as lasting changes to an organism's phenotype induced by the conditions experienced during early development.[12–14] Therefore, in this context, early exposure to increased temperatures associated with warming or MHWs can give rise to phenotypic changes that persist even when temperature stress ceases.[15] These lasting changes may prime individuals for later temperature stress, and are underpinned by altered gene expression profiles, likely driven by developmental epigenetic reprogramming.[16,17] However, as developmental exposure to elevated temperatures has been observed to induce acclimation,[18,19] has no influence on acclimation,[19,20] or has lasting harmful effects,[21,22] the possible consequences and acclimatory potential of developmental exposure are currently unclear.

Genomic studies provide a method for investigating the mechanisms underpinning physiological responses to warming and acclimatory processes. However, a major limitation of previous work on fish is that RNA-Seq is mostly conducted on a single tissue,[23,24] therefore assessing a fraction of the overall molecular response. Nevertheless, studies indicate that the transcriptomic response of fish to elevated temperature is tissue-specific, with different tissues showing variability in the number of genes and functions impacted.[25,26] For example, the brain often exhibits a relatively low number of differentially expressed genes (DEGs); however, important functions such as neurotransmission and oxygen transport are affected.[26–28] Other commonly studied tissues include gills, which display alterations to protein processing and immune response,[25,28] and muscle that show the disruption of metabolic processes and immune response.[29,30] However, beyond these commonly studied tissue-types, vital tissues such as the intestine have received limited attention,[31] whilst niche tissues such as the spleen have been subjected to outdated assessments.[32] The heart has also received limited research attention to date, despite physiological measurements demonstrating the impacts warming can have on cardiovascular functioning.[33] Conversely, the liver has been the primary subject of molecular research in the context of climate change. This focus stems from widespread physiological observations of

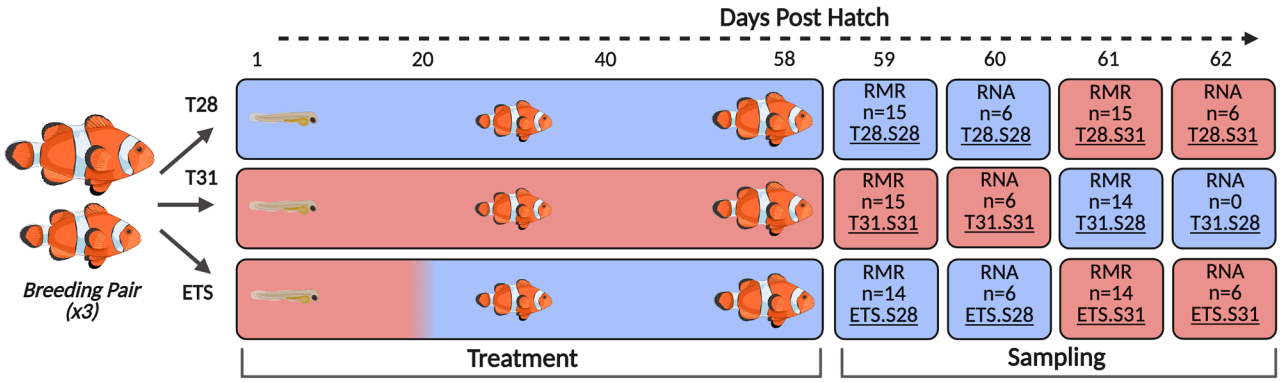

Figure 1. Experimental design displaying the treatment and sampling structure

Color indicates treatment/sampling temperature, with blue representing 28°C and red representing 31°C. Fish were in either 28°C (T28), 31°C (T31), or early-life thermal stress conditions (ETS) until 58 days post hatch. From 59 days post hatch individuals were tested at either 28°C (S28) or 31°C (S31). Final experimental group labels are underlined in the sampling section.

increased metabolic costs in fish at elevated temperatures, with metabolic disruption expected to be the primary driver of detrimental phenotypes under future warming.[34–36] The liver often exhibits a relatively high number of DEGs characterized by alterations to metabolic and immune response pathways.[24,25] Although liver studies cite metabolic processes as being affected by temperature change,[37,38] rarely do they investigate discrete metabolic pathways such as glycolysis (+2 ATP), the tricarboxylic acid (TCA) cycle (+2 ATP), and oxidative phosphorylation (+32 ATP), each of which differs in its contribution to the energetic status of the fish.[39] Furthermore, owing to the common single-tissue approach, studies have yet to provide an integrated multi-tissue assessment of metabolic changes in fish, and the role of tissues regulating energetic substrates is currently unknown. For example, pancreatic insulin regulates glucose uptake and utilization in multiple tissues, and is thus central to organismal consumption and storage of energy.[40] Yet, while altered insulin sensitivity has been observed in vertebrates under heat stress,[41] the importance of insulin regulation in response to warming in fish is yet to be studied.

To our knowledge, no study to date has conducted multi-tissue transcriptomic analyses (> four tissues) of fish in the context of climate change, whilst studies of crucial early-life stages are also limited. Here, we investigate how early-life stage fish (~60 days post hatch) respond to temperatures associated with ocean warming and MHWs, by sequencing seven tissues of 30 *Amphiprion ocellaris* individuals. This transcriptomic data is coupled with measurements of wet-weight and routine metabolic rate (RMR), allowing for comparisons between metabolism/size and molecular trends. Moreover, utilizing an experimental design comprising six thermal regimes, with three treatments (T:28°C constant, 31°C constant, and 31°C Early-life Thermal Stress: ETS) and two sampling temperatures (S:28°C and 31°C), this study aims to investigate the chronic, acute, and acclimatory effects of elevated temperature on fish (Figure 1). Specifically, it aims to investigate if larval and/or larval-juvenile exposure to +3°C reduces the effect of elevated temperature on metabolic rates at 60 dph. At the molecular level, it aims to identify biological processes associated with thermal stress/acclimation across a range of tissues, with a focus on identifying changes to discrete anabolic/catabolic pathways across tissues. Finally, it aims to elucidate the currently unknown molecular response of the pancreas to thermal stress. Based on this approach we hypothesize that: (i) acute and chronic exposure to +3°C will increase metabolic rates, (ii) early-life exposure to 31°C will reduce the effects of +3°C on metabolic rates of ~60 dph fish, (iii) tissues will display unique changes to a range of biological processes including those related to immunity, metabolism, and neural functioning at +3°C, and (iv) any observed metabolic acclimation will be driven by energetic changes/regulation in the liver and pancreas.

Overall, the multi-tissue transcriptomic results identified reprogramming of metabolic pathways throughout the body under differing thermal regimes, particularly in the liver-pancreas axis. Specifically, larval-juvenile +3°C exposure induced the developmental acclimation of metabolic rates and caused the upregulation of oxidative phosphorylation (liver) and downregulation of insulin secretion (pancreas). Therefore, this comprehensive multi-tissue assessment indicates that changes to core molecular pathways in the liver-pancreas axis may underpin successful acclimation to warming in fish.

RESULTS

Physiological response

The RMR of juvenile *A. ocellaris* was not affected by 1–58 dph treatment (T28, T31, or ETS) ($F = 0.139$, $p = 0.870$) (Table S1), with only an 11.8% increase in mean RMR between T28.S28 and T31.S31. However, RMR increased when fish were sampled at 31°C ($F = 14.782$, $p < 0.01$) (Figure 2). Fish raised in the T28 treatment displayed the greatest increase in mean RMR as sampling temperature increased (22.3%), whilst fish in the ETS and T31 treatments exhibited 16.9% and 4.6% increases in mean RMR at S31 (Figure 2). As such, there was a significant interaction between treatment and sampling temperature ($F = 4.61$, $p < 0.05$). Post-hoc pairwise comparisons indicated that only T28.S31vT28.S28 ($T = -4.047$, $p < 0.01$) and ETS.S31vT28.S28 ($T = -3.942$, $p < 0.01$) displayed a significant increase in

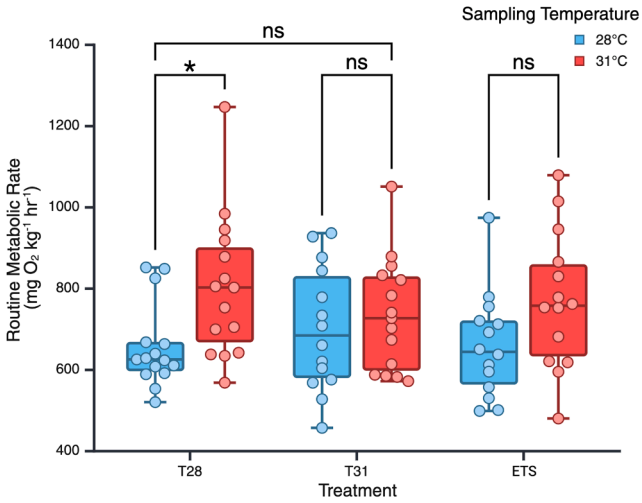

Figure 2. Routine metabolic rates of juvenile *A. ocellaris*

Routine metabolic rate (RMR) of 59 and 61 dph *A. ocellaris* measured via intermittent respirometry. Data points show RMR per individual with median displayed per box and whiskers displaying interquartile range. Figure displays the six experimental groups from left to right: T28.S28, T28.S31, T31.S28, T31.S31, ETS.S28, and ETS.S31 assessed here. Selected results from lsmeans Tukey's pairwise comparisons displayed. * = $p < 0.05$, ns = not significant.

RMR (Table S2). The wet-weight of *A. ocellaris* did not vary between treatments (F = 2.625, $p = 0.080$) (Figure S1; Table S3).

Tissue-specific transcriptomic response

The number of DEGs at elevated temperatures varied between tissue types. For example, the brain, gill, and intestine displayed between 57 and 127 DEGs, the heart and muscle displayed 114–283 DEGs, and the liver and pancreas exhibited 180–801 DEGs across all contrasts (Figure 3). Tissue-specific responses were also highlighted by the low number of common DEGs between different tissue/contrast combinations (Table S4). For example, comparisons of DEGs between the brain-gill and muscle-intestine show <11 common DEGs for each of the four contrasts. Furthermore, despite the high number of DEGs in the liver in T28.S31vT28.S28 (601), no more than 49 were common with any other tissue type in the same contrast. Similarly, of the 801 DEGs in the pancreas in ETS.S28vT28.S28, no more than 63 were in common with any other tissue type in the same contrast (Table S4).

Tissue-specific functional enrichment analysis

Functional enrichment analysis revealed similar tissue-specific results as biological functions were unique to each tissue type (Tables S5, S6, S7, S8, S9, S10, S11, S12, S13, S14, S15, S16, S17, S18, S19, S20, S21, S22, S23, S24, S25, S26, S27, S28, S29, S30, S31, S32, and S33). Furthermore, the majority of GO terms primarily occurred in one or two contrasts within each tissue (Figure S2A), demonstrated by low GO term *p*-value correlations between within-tissue contrasts (Figure S2B). The brain showed changes to the collagen-containing extracellular matrix (ECM), as this GO term appeared in all contrasts apart from T28.S31vT28.S28, with DEGs including collagen (T31.S31vT28.S28, T28.S31vT28.S28, ETS.S28vT28.S28), galectin (T31.S31vT28.S28, ETS.S31vETS.S28, ETS.S28vT28.S28), and vitronectin (ETS.S31vETS.S28). Similar to the brain, many ECM genes were impacted across different contrasts in the liver, with collagen alpha chain proteins strongly altered in all but T28.S31vT28.S28. Furthermore, GO analysis of the liver revealed the unique enrichment of "liver regeneration" in T31.S31vT28.S28 (Figure 3). The gill displayed many enriched GO terms and genes related to cellular transport processes. For example, "symporter activity" (T31.S31vT28.S28), "positive regulation of calcium ion import" (T28.S31vT28.S28, ETS.S28vT28.S28) and "transport across blood-brain barrier" (ETS.S31vETS.S28) were enriched, with genes such as solute carriers' family 13/19 (T28.S31vT28.S28, ETS.S31vETS.S28), family 22 (T31.S31vT28.S28, T28.S31vT28.S28, ETS.S31vETS.S28), family 35 (T31.S31vT28.S28, T28.S31vT28.S28), extracellular calcium receptors (T28.S31vT28.S28, ETS.S28vT28.S28), sodium/calcium exchangers (ETS.S31vETS.S28), sodium- and chloride-dependent transporters (T31.S31vT28.S28, ETS.S31vETS.S28) and amino acid transporters affected (all contrasts). The intestine exhibited strong changes in the expression of genes involved in muscular contraction, with all contrasts exhibiting the enrichment of the "muscle contraction" and "muscle cell fate commitment" GO terms. Furthermore, all contrasts displayed the differential expression of genes related to intestinal mucosa and barrier integrity, with mucins upregulated in all contrasts other than T28.S31vT28.S28, and soluble guanylate cyclase (all contrasts), pro-epidermal growth factor (T28.S31vT28.S28, ETS.S31vETS.S28, ETS.S28vT28.S28), and creatine kinase (ETS.S31vETS.S28) exhibiting various changes in expression.

Tissue-wide metabolic reprogramming

Across all contrasts in the pancreas, we identified 186 DEGs involved in insulin synthesis and secretion (Table S34; Figure S3). These 186 DEGs generally exhibited the highest expression in T28.S28 and the lowest expression in T31.S31, with 184 out of 186 genes showing comparatively lower expression in T31.S31 (Figure S3). Groups with intermediate levels of temperature exposure (T28.S31, ETS.S28, and ETS.S31) exhibited counts between these two extremes. Additionally, 20 of these compiled genes mapped to the insulin secretion KEGG pathway (Figure 4), with all 20 significantly downregulated in T31.S31vT28.S28. Beyond the pancreas, we identified 44 DEGs with functions related to gluconeogenesis, glycogenolysis, glycolysis, glycogenosis, glucose transport, and lactate metabolism across tissues/contrasts (details of genes and their significant up/down regulation in relation to each contrast are specified in Table S35). Genes involved in glucose transport were predominantly downregulated at elevated temperatures, with a *glut4* regulator downregulated in muscle and gills, *glut-1* and *sglt5* downregulated in the pancreas, and *glut2* exhibiting up and down regulation in the heart (Figure 3; Table S35). Conversely, genes involved in gluconeogenesis, glycogenolysis, glycolysis, and glycogenosis exhibited varying levels of up/down regulation across tissues/contrasts (Table S35). We also identified 46 DEGs associated with oxidative phosphorylation that were significantly upregulated in the liver in T31.S31vT28.S28 (Figure 5; Table S36).

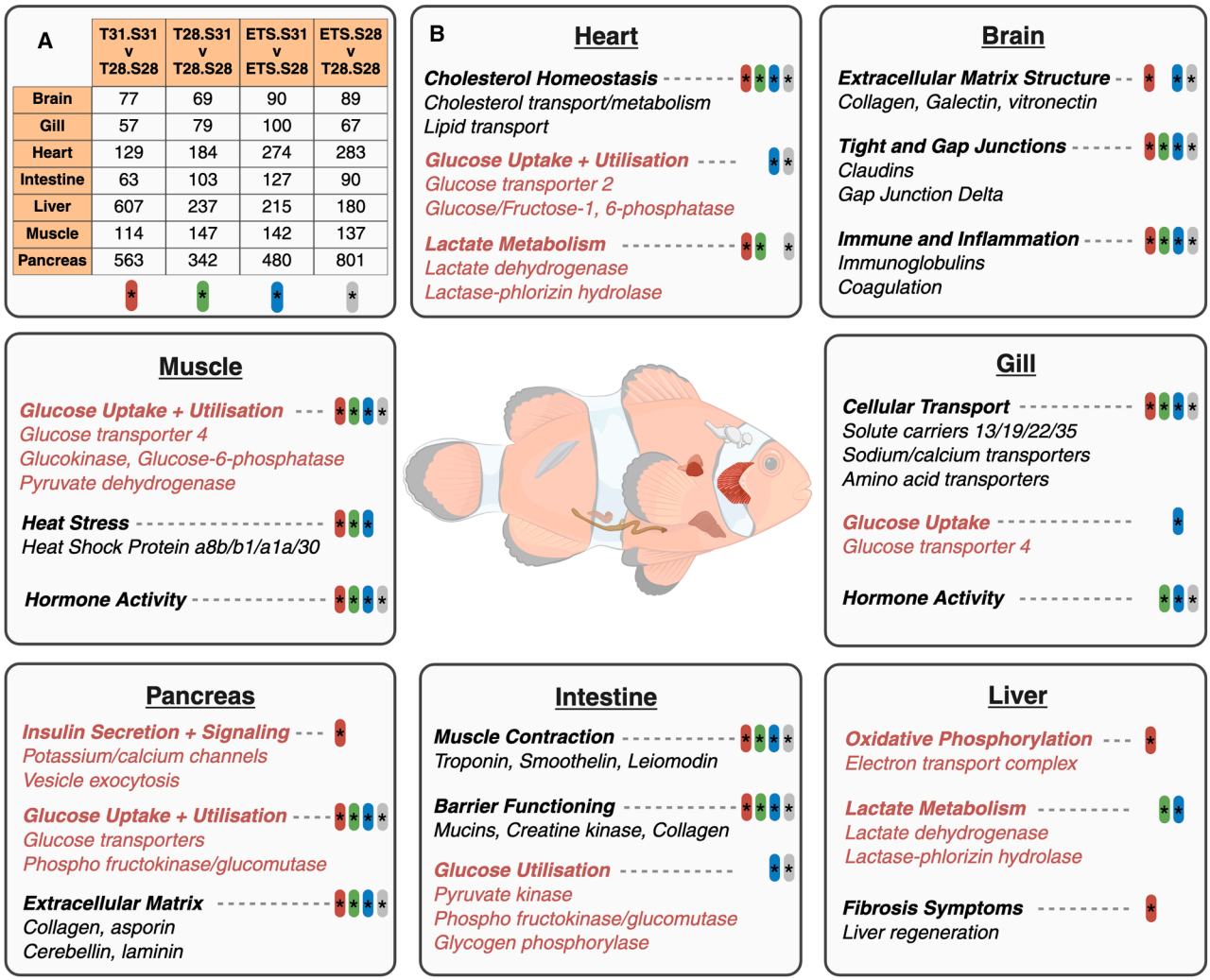

Figure 3. Multi-tissue transcriptional response of *A. ocellaris* to various thermal regimes

(A) Number of differentially expressed genes in brain, gill, heart, intestine, liver, muscle, and pancreas for four different contrasts of experimental groups.

(B) Results presented here are based on DEGs, and functional analyses (GO and KEGG) of T31.S31vT28.S28, T28.S31vT28.S28, ETS.S31vETS.S28, and ETS.S28vT28.S28 contrasts. Color key displays significant ($p < 0.05$) changes of genes/GO/KEGG terms related to the specified function in each contrast. Color and associated contrast are displayed in the table columns in (A). Red text highlights biological functions involved with metabolic processes, including glucose regulation and utilization.

DISCUSSION

Through this multi-tissue transcriptomic analysis of a fish, we demonstrate that both developmental and sampling temperature influence the metabolic and molecular response of *A. ocellaris* to ocean warming, with the molecular response being highly tissue-specific. Such tissue-specificity is observed in the varying number of DEGs and differing enriched biological functions between tissues. Previous transcriptomic assessments of fish and warming have also reported strong tissue-specificity, as studies assessing the response of a few tissues (a combination of gill, liver, muscle, brain, and fin, $\leq$ three tissues) to elevated temperature show <119 genes are common across three tissue types, with the biological functions of DEGs differing between tissues.[42–45] Furthermore, our recent study[46] demonstrated that the brain, liver, muscle, and digestive tract of 20 dph *A. ocellaris* display distinct expression profiles at 31°C. Here, tissue-specific differences in ~60 dph *A. ocellaris* were dominated by strong effects of temperature on the liver-pancreas axis, demonstrated by the high number of DEGs in these tissues.

In contrast to the overall trend of this study, *A. ocellaris* weights displayed a uniform response across all treatments, indicating growth was not affected by temperature. Previous studies show faster or slower growth in fish at elevated temperatures, both of which contrast with the null effect observed here.[47,48] More specifically, our results oppose observations made in Moore et al.,[49] whereby larval *A. ocellaris* displayed faster growth under the same level of temperature change. A trend that is also observed in larvae of other fish species.[50,51]

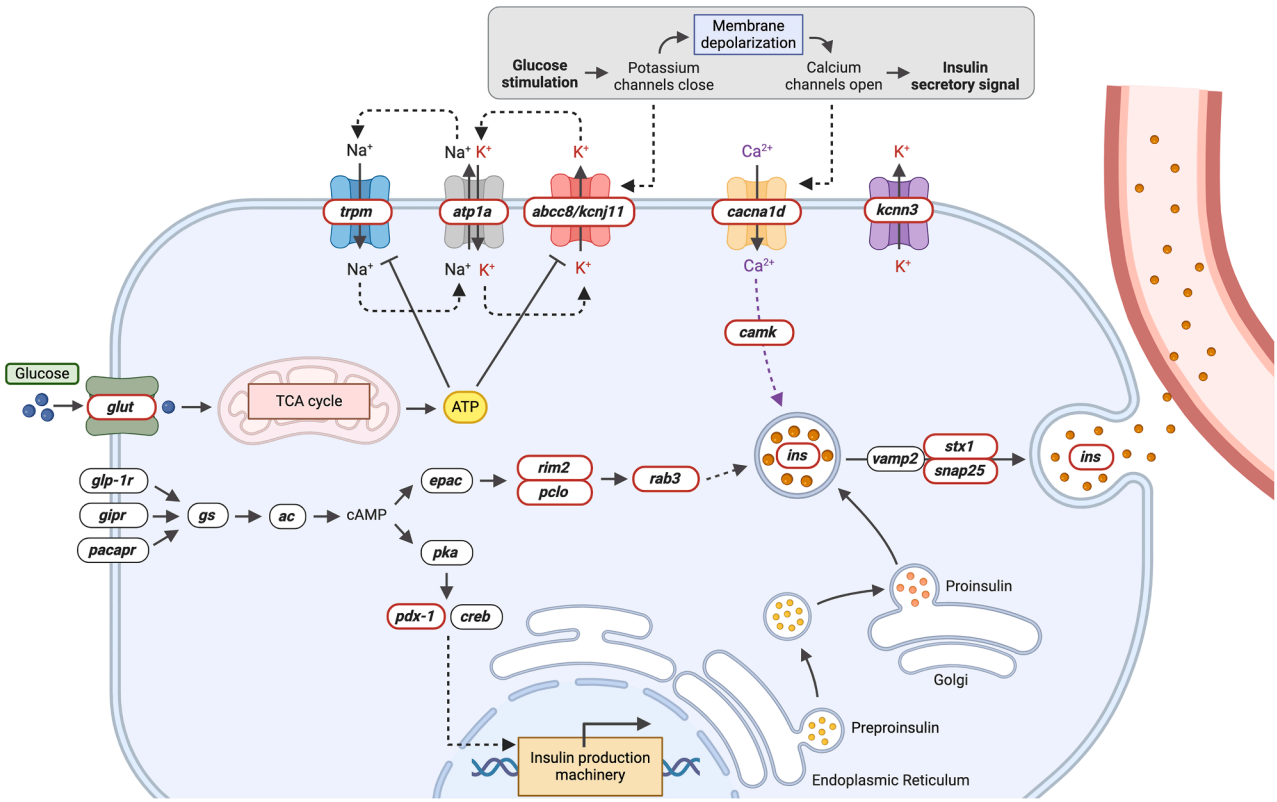

Figure 4. Transcriptomic changes to the insulin secretion pathway in the pancreas

Modified version of the "insulin secretion" KEGG pathway within pancreatic cells. Bold/italic symbols represent genes within the pathway. Genes with a black outline were not differentially expressed, whereas genes with a red outline were significantly downregulated ($p < 0.05$) in the T31.S31 group compared to the T28.S28 control.

Therefore, it is likely that size differences existing at 20 dph at 31°C are mitigated between 20 and 60 dph. This is ecologically understandable as following growth driven pelagic larval stages, juvenile *A. ocellaris* recruit to anemones where they enter a size-based social hierarchy. Here, they enter as a small non-breeder with their growth and maturation restricted by the threat of eviction from individuals occupying higher social positions.[52] Therefore, if size/weight differences at 20 dph did exist here (as observed in Moore et al.[49]), it is expected that these size differences would level out through the juvenile period, as the size ceilings associated with juvenile non-breeding societal positions would allow initially smaller individuals to catch up.

Although weight displayed no change, elevated temperature increased RMR, with the effect varying amongst experimental groups. Similar increases in metabolic rates have been observed in multiple species of fish,[34,35,53,54] with its increase hypothesised to reduce energy available for non-essential functions such as reproduction and growth.[55] However, in contrast to previous studies and our initial hypothesis, we did not observe increased RMR following chronic temperature stress (59 days-T31.S31vT28.S28), only following acute stress (1 day-T28.S31vT28.S28). Furthermore, we found that the impact of measuring RMR at 31°C was reduced with increasing developmental exposure to 31°C. As hypothesised, these results suggest that at these temperatures, *A. ocellaris* may experience metabolic developmental acclimation to temperature stress following larval-juvenile exposure to +3°C. Such acclimation to environmental stress has been demonstrated in multiples species, with phenotypic traits such as reproduction and growth recovering with larval exposure.[19,56] Resultingly, the restoration of natural phenotypes through rapid developmental acclimation is proposed to be one way in which fish may survive in a changing ocean.

In line with these RMR measurements, the transcriptomic data here highlight metabolic reprogramming in multiple tissues, particularly in the liver-pancreas axis. Together, these metabolic and transcriptomic changes indicate that developmental programming underpinned by gene expression changes may lead to phenotypic changes later in life. Similar molecular alterations to metabolic processes have been observed in multiple fish species at elevated temperatures;[23,37,57] however, these studies often document metabolic changes in a single tissue type,[27,29,42] and have never observed such changes in the pancreas. Here, multiple genes involved in glycolysis (*pk* and *pfk*), gluconeogenesis (*grhpr* and *fbp*), glycolysis/gluconeogenesis (*pgam* and *gapdh*), glucose transport (*glut1/2/9* and *trarg1a*), and glycogenolysis/gluconeogenesis (*g6pc*) display altered expression in multiple tissues. The absence of a uniform

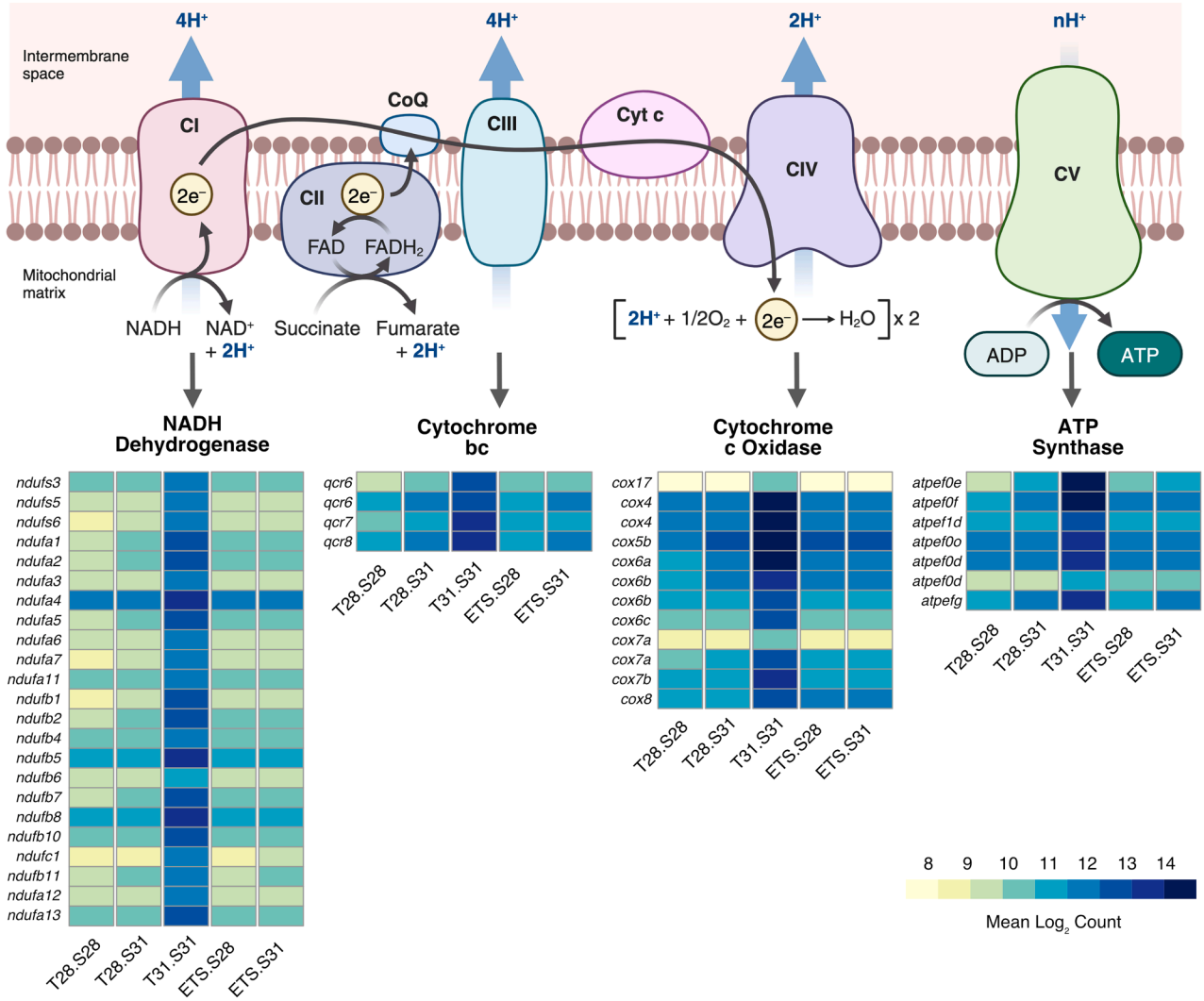

Figure 5. Transcriptomic changes to the oxidative phosphorylation pathway in the liver

Diagram depicting the process of electron transport and oxidative phosphorylation that occurs within the mitochondrial membrane. Heatmaps display the DESeq2 normalized mean (plus one) $\log_2$ counts of 46 DEGs ($p < 0.05$) identified in the liver within the T31.S31vT28.S28 contrast, with counts displayed for each of the five experimental groups. The four heatmaps are positioned according to the function of the genes within the electron transport chain. From left to right, Complex I: NADH dehydrogenase, Complex III: Cytochrome *bc*1, Complex IV: Cytochrome *c* oxidase, and Complex V: ATP synthase.

response across all tissues/thermal regimes is likely underpinned by the unique role of each tissue in metabolism and the multifunctional enzymes involved, with metabolomic measurements of end products needed to resolve such trends (as in Zhu et al.[58]). Nonetheless, tissue-wide changes to the expression of 44 genes associated with glucose transport, utilization, and synthesis clearly indicate that warming induces transcriptional metabolic reprogramming of carbohydrate utilization. As tissue-wide activity of these processes influence glucose availability and energy production, such altered expression of these genes may impact fitness.[54,59] However, further studies using techniques such as proteomics/metabolomics are required to confirm these preliminary mRNA based molecular trends, with additional phenotyping including advanced morphological measurements (hepatosomatic index, gonadosomatic index, and condition factor), further physiological testing (critical thermal maxima, immunity, and cardiac output), and behavioral assays, required to validate the trends observed here.

We also observed a decoupling of metabolic and transcriptomic results as oxidative phosphorylation genes were upregulated without an increase in RMR (T31.S31), yet they also displayed no change with an increase in RMR (T28.S31). These unexpected trends are likely driven by the simplicity of common phenotypic proxies for metabolism (RMR), which rely solely on oxygen consumption measurements. However, metabolism at the molecular level is inherently more complex, evidenced by the array of agonistic/antagonistic pathways and multifunctional enzymes used to generate cellular energy and metabolic products. For example, in addition to glucose, other monosaccharides, lipids, and amino acids are used to generate ATP in

fish,[60,61] with switches to lipid metabolism reported in fish at elevated temperatures.[24,38,39] Similar switches in metabolic pathways may underpin the significant increase in RMR observed in T28.S31, as this group alone shows strong the upregulation of lactate dehydrogenase (*ldhbb*) and the lactate/pyruvate transporting monocarboxylate transporter (*slc16a1*) in the liver. This paradoxically suggests an increase in both anaerobic and aerobic metabolism under acute temperature stress. Therefore, it is possible that increased oxygen consumption in T28.S31 fish led to local oxygen deficiencies within the liver, activating anaerobic pathways in an oxygen-limited microenvironment.[62] Such an approach would allow continued ATP production when oxygen is reduced locally due to increased energy demand and limited cardiovascular capacity.[63] Alternatively, as lactate dehydrogenase can convert lactate to pyruvate and as lactate may represent a "universal fuel" for metabolism,[64,65] *ldhbb* and *slc16a1* upregulation may indicate a switch to aerobic lactate metabolism, occurring independently or simultaneously with anaerobic metabolism. Such switches would allow for more rapid energy production, as lactate directly enters more efficient ATP production pathways.[64,65] Further studies utilizing targeted enzyme assays, or direct measurements of lactate from blood, should be conducted to confirm such switches to anaerobic metabolism.

Another signal of metabolic reprogramming is observed in the pancreas, as 184 DEGs associated with insulin synthesis and secretion were downregulated following chronic +3°C exposure. Within pancreatic cells, glucose-driven ATP production closes membrane bound transient receptor potential and potassium channels, inducing an influx of extracellular calcium, which triggers the exocytosis of insulin-containing secretory granules.[66] Therefore, ion channels are integral to insulin secretion, and here we observed the downregulation of such ion channel genes (*trpm, atp1a, abcc8, kcnj11, cacna1d,* and *kcnn3*). Furthermore, genes involved in both vesicle trafficking (*rim2a, pclo,* and *rab3*) and the vesicle exocytic SNARE complex (*stx1* and *snap25*)[66] were downregulated, while insulin promoter factor *pdx-1* as well as *ins* itself were also downregulated. Overall, these results indicate that insulin synthesis and secretion machinery in the pancreas is transcriptionally suppressed under chronic +3°C exposure (T31.S31), with reduced exposure to +3°C (T28.S31, ETS.T28, and ETS.S31) inducing intermediate effects. Interestingly, as energetic demands increase at higher temperatures, this observed suppression of insulin secretion opposes a predicted increase in insulin secretion that would promote glucose uptake and energy production;[67] therefore, these results may represent a previously undocumented temperature-stress response mechanism.

Although blood glucose levels were not monitored in this study, fish exposed to high temperatures did not exhibit extensive physiological differences (mortality, weight, and symptoms of hyper/hypoglycemia), so it is likely that blood glucose levels varied within the biologically defended level of glycemia (BDLG).[68,69] Therefore, based on the strong transcriptomic trends here, we hypothesize that the downregulation of insulin secretion following chronic exposure to 31°C may be a mechanism of within-generation developmental acclimation, utilized to maintain blood glucose levels within the normal physiological range despite increased energy/glucose demand. However, future studies pairing a similar transcriptomic approach with measurements of blood glucose levels are required to confirm such a hypothesis. Nonetheless, altered insulin output in response to heat stress has been documented in other species, including pigs and cattle,[70,71] and the acclimation temperature of ectothermic frogs has been demonstrated to alter the metabolic response of muscles to insulin.[72] Furthermore, adaptive insulin resistance is employed by nutrient limited cavefish to keep blood glucose levels high and increase body weights.[73] Such studies report both increased insulin output and alterations to insulin sensitivity in response to heat stress; however, our study provides transcriptomic evidence of an organism utilizing insulin secretion suppression as an acclimatory response to temperature stress.

A coupling of insulin secretion suppression with increased oxidative phosphorylation was found in the liver-pancreas axis of T31.S31 fish. This upregulation of oxidative phosphorylation may represent a shift toward a high ATP-yield metabolic pathway, or a compensatory mechanism that maintains ATP output despite the reduced electron transport efficiency associated with increased temperatures.[74] When aligned with the acclimation of metabolic rates in T31.S31 fish, we extend our hypothesis to suggest that reduced insulin secretion and increased oxidative phosphorylation may represent complementary acclimatory processes within the liver-pancreas axis. Proposing that while insulin suppression reduces glucose uptake and maintains critical BDLG despite higher energetic demands, increased oxidative phosphorylation compensates for reduced glucose uptake by maximizing ATP production from each glucose molecule. Therefore, used together these acclimatory processes sustain ATP output and maintain critical BDLG, thus alleviating any negative effects on overall fitness. This metabolic remodeling, mainly driven by the liver-pancreas axis, appears to prevent the common metabolic changes observed in fish at higher temperatures in T31.S31 fish and may alleviate the impacts of heat stress in the future. However, the suitability of this mechanism in negating the effects of longer-term ocean warming is unknown, as sustained insulin suppression may give rise to symptoms akin to those of diabetes,[69] while excessive oxidative phosphorylation will increase the production of reactive oxygen species that can damage vital cell components.[75] Additionally, it appears that only chronic larval-juvenile +3°C exposure induces our hypothesized acclimatory mechanism, as these molecular changes were not observed in ETS.S31 fish. Together, the transcriptomic changes observed here support our initial hypothesis that energetic regulation in the liver and pancreas will underpin metabolic acclimation in fish, resulting in our proposed hypothesis of liver-pancreas driven remodeling. However, as this model is based upon transcriptomic evidence and a single physiological phenotype, further testing of this hypothesis is required.

Beyond the reprogramming of metabolic processes, different tissues displayed unique changes to other biological processes. For example, the liver displayed signs of potential liver fibrosis/damage, evidenced by increased collagen deposition and extracellular matrix (ECM) restructuring.[76] Previous studies have reported similar liver damage in thermally challenged fish,[77,78] with such changes leading to loss of appetite and body

weakness, both of which can have detrimental impacts on overall fitness.[79] However, as fish that only experienced acute temperature stress displayed limited signs of fibrosis, while fish experiencing developmental exposure to +3°C display multiple signs, our results suggest that developmental exposure induces fibrosis-like symptoms. Similarly, early developmental exposure to +3°C may influence the expression of ECM related genes in the brain, as all contrasts other than T28.S31vT28.S28, exhibited the enrichment of "collagen-containing extracellular matrix". As the ECM structure is important for neural development and collagen has roles in neural maturation and synaptic differentiation,[80,81] developmental exposure to +3°C may also alter *A. ocellaris* brain development. Together, these results in the liver and brain emphasize that although developmental exposure may have potential acclimatory benefits, these benefits may be offset by lasting negative effects on other processes.

One tissue that displayed similar alterations to biological processes across experimental groups was the intestine, with biological functions related to muscle contraction enriched in all contrasts. The intestinal tract contains smooth muscle cells that are primarily involved in the propulsion and mixing of food, facilitating the digestion and absorption of nutrients.[82] Thus, here, temperature stress appeared to change muscle contractability within the intestine of *A. ocellaris*, potentially affecting food motility. Previous studies have demonstrated that smooth muscle contractability in multiple fish is altered at elevated temperatures;[83,84] however, the physiological consequences of these changes remain uncertain. Beyond propulsion and mixing, the intestine is a key barrier to the external environment and is therefore involved in electrolyte balance and immune defense.[85] We observed the altered expression of multiple genes related to intestinal mucosa and barrier integrity across the different contrasts, indicating that future temperature change may affect these vital processes. Specifically, intestinal mucosa acts as a physical barrier involved in immune defense,[86] therefore compromised barrier functionality could provide a potential point of entry to harmful bacteria, stimulating the previously documented upregulation of immune pathways at elevated temperatures.[23,30]

The gill was another tissue that displayed similar trends across contrasts, as many genes related to transport were differentially expressed. For example, solute carriers (*slc*), including families *13/19/22/35* and sodium-dependent transporters, including *b(0)at1* and *xtrp3* were strongly downregulated in T31.S31, T28.S31, and ETS.S31 fish, indicating that +3°C induces the downregulation of transport related genes in the gills regardless of thermal history. The downregulation of solute carriers involved with folate/thiamine (*slc19*), organic cation/anion/zwitterions (*slc22*), and nucleoside-sugar transport (*slc35*), as well as Na +–sulfate/carboxylate cotransport (*slc13*), suggest that vital functions of the gills such as osmoregulation, the excretion of nitrogenous waste and pH regulation[87,88] may be altered at elevated temperatures. Similar changes to transport processes have previously been documented in a broad range of fish taxa,[89,90] evidencing that solute transport in fish gills is altered at the transcriptomic level by warming.

Overall, this study indicates that fish will exhibit metabolic and molecular changes as ocean temperatures increase, with multiple biological processes impacted across different tissue types. Specifically, fish RMR is affected by a +3°C temperature increase, and tissues exhibit unique molecular changes at +3°C. We demonstrated that the duration and timing of exposure can mediate temperature effects, with chronic larval-juvenile exposure inducing the developmental acclimation of metabolic rates at +3°C. Transcriptionally, we observed the reprogramming of metabolic processes across multiple tissues. Specifically, chronic +3°C exposure induced the upregulation of oxidative phosphorylation (liver) and downregulation of insulin secretion (pancreas). When aligned with the observed developmental acclimation of metabolic rates, we hypothesize that these complementary changes to oxidative phosphorylation and insulin secretion in the liver-pancreas axis may represent core processes underpinning acclimation. This previously undocumented mechanism may help regulate the increased energetic demands placed on fish by future ocean warming and marine heatwaves.

Limitations of the study

Here, developmental acclimation to warming in clownfish is investigated through metabolic measurements and transcriptomic sequencing. Although metabolism is widely assessed in fish biology, and changes in metabolism are linked to ecological outcomes, measuring the effects of +3°C on other aspects of physiology (e.g., survival and growth) is required to confirm the observed acclimation across longer-term timescales. Similarly, the molecular mechanisms described here are primarily based on transcriptomic data and thus require validation through further molecular phenotyping. For example, direct measurements of blood sugar, insulin, and oxidative phosphorylation are required to confirm the mechanisms of adaptation postulated here. Finally, we note that this study is based on a single level of temperature increase (+3°C) and a single species of fish (*Amphiprion ocellaris*); therefore, further experimentation with other species/temperatures is required to prove the wider applicability of the results/hypothesis.

RESOURCE AVAILABILITY

Lead contact

Requests for further information and resources should be directed to and will be fulfilled by the lead contact, Billy Moore (bcm9945@nyu.edu).

Materials availability

This study did not generate new unique reagents.

Data and code availability

All transcriptomic sequencing reads have been deposited in the NCBI database under the BioProject ID Database: PRJNA1094601. All data and code can be accessed at: http://datadryad.org/share/6Q1S04EK0q3dnnkxdMeEs3HeRlx4RkT8GIg5xHZ0fOE.

ACKNOWLEDGMENTS

We thank Erina Kawai for the collection and Gelyn Bourguignon (OIST) for the rearing of *A. ocellaris* breeding pairs. Research reported in this publication was supported by funding from the Okinawa Institute of Science and Technology as well as a Japan Society for the Promotion of Science DC1 fellowship and KAKENHI (Project Number: 21H03655).

AUTHOR CONTRIBUTIONS

Conceptualization: BM, TR1 (Timothy Ravasi), and TR2 (Taewoo Ryu).
Experimental Design and Set-up: BM and SM.
Metabolic Measurements: BM and SM.
Micro-dissections: BM and MI.
Data Analysis and Visualization: BM and TR2.
Writing—original draft: BM and TR2.
Writing—review and editing: BM and TR2.

DECLARATION OF INTERESTS

Authors declared no competing interests.

STAR★METHODS

Detailed methods are provided in the online version of this paper and include the following:

- KEY RESOURCES TABLE
- EXPERIMENTAL MODEL AND STUDY PARTICIPANT DETAILS
- METHOD DETAILS
  - Experimental design
  - Larval-juvenile rearing
  - Physiological measurements
  - RNA sequencing sampling
  - Nucleic acid extraction and sequencing
- QUANTIFICATION AND STATISTICAL ANALYSIS
  - Physiology: Statistical analyses
  - RNA-sequencing: Bioinformatic analysis

SUPPLEMENTAL INFORMATION

Supplemental information can be found online at https://doi.org/10.1016/j.isci.2025.113395.

Received: March 28, 2025
Revised: July 2, 2025
Accepted: August 14, 2025
Published: August 19, 2025

REFERENCES

1. Pörtner, H.-O., Roberts, D.C., Poloczanska, E.S., Mintenbeck, K., Tignor, M., Alegría, A., Craig, M., Langsdorf, S., Löschke, S., Möller, V., and Okem, A. (2022). IPCC, 2022: Summary for Policymakers. In Climate Change 2022: Impacts, Adaptation, and Vulnerability. Contribution of Working Group II to the Sixth Assessment Report of the Intergovernmental Panel on Climate Change (Cambridge University Press), pp. 3–33. https://doi.org/10.1017/9781009325844.001.
2. Oliver, E.C.J., Benthuysen, J.A., Darmaraki, S., Donat, M.G., Hobday, A.J., Holbrook, N.J., Schlegel, R.W., and Sen Gupta, A. (2021). Marine heatwaves. Ann. Rev. Mar. Sci *13*, 313–342.
3. Frolicher, T.L., Fischer, E.M., and Gruber, N. (2018). Marine heatwaves under global warming. Nature *560*, 360–364. https://doi.org/10.1038/s41586-018-0383-9.
4. Lee, H., Calvin, K., Dasgupta, D., Krinner, G., Mukherji, A., Thorne, P., Trisos, C., Romero, J., Aldunce, P., and Barret, K. (2023). In IPCC, 2023: Climate Change 2023: Synthesis Report, Summary for Policymakers. Contribution of Working Groups I, II and III to the Sixth Assessment Report of the Intergovernmental Panel on Climate Change [Core Writing Team, H. Lee and J. Romero, eds. (IPCC).
5. Dahlke, F.T., Wohlrab, S., Butzin, M., and Pörtner, H.-O. (2020). Thermal bottlenecks in the life cycle define climate vulnerability of fish. Science *369*, 65–70.
6. Munday, P.L., McCormick, M.I., and Nilsson, G.E. (2012). Impact of global warming and rising CO_2 levels on coral reef fishes: what hope for the future? J. Exp. Biol. *215*, 3865–3873.
7. Donelson, J.M., Munday, P.L., McCormick, M.I., Pankhurst, N.W., and Pankhurst, P.M. (2010). Effects of elevated water temperature and food availability on the reproductive performance of a coral reef fish. Mar. Ecol. Prog. Ser. *401*, 233–243. https://doi.org/10.3354/meps08366.
8. Malavasi, S., Cipolato, G., Cioni, C., Torricelli, P., Alleva, E., Manciocco, A., Toni, M., and Fusani, L. (2013). Effects of Temperature on the Anti-predator Behaviour and on the Cholinergic Expression in the European Sea Bass (Dicentrarchus labraxL.) Juveniles. Ethology *119*, 592–604. https://doi.org/10.1111/eth.12100.
9. Rodgers, G.G., Donelson, J.M., McCormick, M.I., and Munday, P.L. (2018). In hot water: sustained ocean warming reduces survival of a low-latitude coral reef fish. Mar. Biol. *165*, 73.
10. Campana, S.E., Stefánsdóttir, R.B., Jakobsdóttir, K., and Sólmundsson, J. (2020). Shifting fish distributions in warming sub-Arctic oceans. Sci. Rep. *10*, 16448.
11. Simpson, S.D., Jennings, S., Johnson, M.P., Blanchard, J.L., Schön, P.-J., Sims, D.W., and Genner, M.J. (2011). Continental shelf-wide response of a fish assemblage to rapid warming of the sea. Curr. Biol. *21*, 1565–1570.
12. Barker, D.J. (1992). The fetal origins of diseases of old age. Eur. J. Clin. Nutr. *46*, S3–S9.
13. Rabadan-Diehl, C., and Nathanielsz, P. (2013). From Mice to Men: research models of developmental programming. J. Dev. Origin. Health Dis. *4*, 3–9.
14. Li, M., Reynolds, C.M., Segovia, S.A., Gray, C., and Vickers, M.H. (2015). Developmental programming of nonalcoholic fatty liver disease: the effect of early life nutrition on susceptibility and disease severity in later life. BioMed Res. Int. *2015*, 437107.
15. Angilletta, M.J., Jr. (2009). Thermal Adaptation: A Theoretical And Empirical Synthesis (Oxford University Press), pp. 1–285.
16. Burggren, W.W. (2019). Phenotypic switching resulting from developmental plasticity: fixed or reversible? Front. Physiol. *10*, 1634.
17. Anastasiadi, D., Díaz, N., and Piferrer, F. (2017). Small ocean temperature increases elicit stage-dependent changes in DNA methylation and gene expression in a fish, the European sea bass. Sci. Rep. *7*, 1–12.
18. Scott, G.R., and Johnston, I.A. (2012). Temperature during embryonic development has persistent effects on thermal acclimation capacity in zebrafish. Proc. Natl. Acad. Sci. USA *109*, 14247–14252.
19. Grenchik, M.K., Donelson, J.M., and Munday, P.L. (2013). Evidence for developmental thermal acclimation in the damselfish, Pomacentrus moluccensis. Coral Reefs *32*, 85–90.
20. Donelson, J.M., McCormick, M.I., Booth, D.J., and Munday, P.L. (2014). Reproductive acclimation to increased water temperature in a tropical reef fish. PLoS One *9*, e97223.
21. Kourkouta, C., Printzi, A., Geladakis, G., Mitrizakis, N., Papandroulakis, N., and Koumoundouros, G. (2021). Long lasting effects of early temperature exposure on the swimming performance and skeleton development of metamorphosing Gilthead seabream (Sparus aurata L.) larvae. Sci. Rep. *11*, 8787.
22. Mateus, A.P., Costa, R.A., Cardoso, J.C.R., Andree, K.B., Estévez, A., Gisbert, E., and Power, D.M. (2017). Thermal imprinting modifies adult stress and innate immune responsiveness in the teleost sea bream. J. Endocrinol. *233*, 381–394.
23. Bernal, M.A., Schunter, C., Lehmann, R., Lightfoot, D.J., Allan, B.J.M., Veilleux, H.D., Rummer, J.L., Munday, P.L., and Ravasi, T. (2020). Species-specific molecular responses of wild coral reef fishes during a marine heatwave. Sci. Adv. *6*, eaay3423.
24. Veilleux, H.D., Ryu, T., Donelson, J.M., van Herwerden, L., Seridi, L., Ghosheh, Y., Berumen, M.L., Leggat, W., Ravasi, T., and Munday, P.L. (2015). Molecular processes of transgenerational acclimation to a

warming ocean. Nat. Clim. Chang. *5*, 1074–1078. https://doi.org/10.1038/nclimate2724.

25. Li, P., Liu, Q., Li, J., Wang, F., Wen, S., and Li, N. (2021). Transcriptomic responses to heat stress in gill and liver of endangered Brachymystax lenok tsinlingensis. Comp. Biochem. Physiol., Part D: Genomics Proteomics *38*, 100791. https://doi.org/10.1016/j.cbd.2021.100791.
26. Zhang, W., Xu, X., Li, J., and Shen, Y. (2022). Transcriptomic analysis of the liver and brain in grass carp (Ctenopharyngodon idella) under heat stress. Mar. Biotechnol. *24*, 856–870.
27. Bernal, M.A., Schmidt, E., Donelson, J.M., Munday, P.L., and Ravasi, T. (2022). Molecular Response of the Brain to Cross-Generational Warming in a Coral Reef Fish. Front. Mar. Sci. *9*, 784418. https://doi.org/10.3389/fmars.2022.784418.
28. Kim, S.Y., Costa, M.M., Esteve-Codina, A., and Velando, A. (2017). Transcriptional mechanisms underlying life-history responses to climate change in the three-spined stickleback. Evol. Appl. *10*, 718–730. https://doi.org/10.1111/eva.12487.
29. Zhao, X., Sun, Z., Xu, H., Song, N., and Gao, T. (2021). Transcriptome and co-expression network analyses reveal the regulatory pathways and key genes associated with temperature adaptability in the yellow drum (Nibea albiflora). J. Therm. Biol. *100*, 103071. https://doi.org/10.1016/j.jtherbio.2021.103071.
30. Molina, A., Dettleff, P., Valenzuela-Muñoz, V., Gallardo-Escarate, C., and Valdés, J.A. (2023). High-Temperature Stress Induces Autophagy in Rainbow Trout Skeletal Muscle. Fishes *8*, 303.
31. Zhou, C., Gao, P., and Wang, J. (2023). Comprehensive Analysis of Microbiome, Metabolome, and Transcriptome Revealed the Mechanisms of Intestinal Injury in Rainbow Trout under Heat Stress. Int. J. Mol. Sci. *24*, 8569.
32. Huang, J., Li, Y., Liu, Z., Kang, Y., and Wang, J. (2018). Transcriptomic responses to heat stress in rainbow trout Oncorhynchus mykiss head kidney. Fish Shellfish Immunol. *82*, 32–40.
33. Eliason, E.J., and Anttila, K. (2017). Temperature and the cardiovascular system. Fish Physiol. *36*, 235–297.
34. Nilsson, G.E., Crawley, N., Lunde, I.G., and Munday, P.L. (2009). Elevated temperature reduces the respiratory scope of coral reef fishes. Glob. Change Biol. *15*, 1405–1412. https://doi.org/10.1111/j.1365-2486.2008.01767.x.
35. Johansen, J.L., and Jones, G.P. (2011). Increasing ocean temperature reduces the metabolic performance and swimming ability of coral reef damselfishes. Glob. Change Biol. *17*, 2971–2979. https://doi.org/10.1111/j.1365-2486.2011.02436.x.
36. McMahon, S.J., Munday, P.L., and Donelson, J.M. (2023). Energy use, growth and survival of coral reef snapper larvae reared at elevated temperatures. Coral Reefs *42*, 31–42.
37. Veilleux, H.D., Ryu, T., Donelson, J.M., Ravasi, T., and Munday, P.L. (2018). Molecular Response to Extreme Summer Temperatures Differs Between Two Genetically Differentiated Populations of a Coral Reef Fish. Front. Mar. Sci. *5*, 349. https://doi.org/10.3389/fmars.2018.00349.
38. Liu, S., Wang, X., Sun, F., Zhang, J., Feng, J., Liu, H., Rajendran, K.V., Sun, L., Zhang, Y., Jiang, Y., et al. (2013). RNA-Seq reveals expression signatures of genes involved in oxygen transport, protein synthesis, folding, and degradation in response to heat stress in catfish. Physiol. Genomics *45*, 462–476.
39. Kohlmeier, M. (2015). Nutrient Metabolism: Structures, Functions, and Genes (Academic Press), pp. 1–825.
40. Rui, L. (2014). Energy metabolism in the liver. Compr. Physiol. *4*, 177–197.
41. Morera, P., Basiricò, L., Hosoda, K., and Bernabucci, U. (2012). Chronic heat stress up-regulates leptin and adiponectin secretion and expression and improves leptin, adiponectin and insulin sensitivity in mice. J. Mol. Endocrinol. *48*, 129–138.
42. Huth, T.J., and Place, S.P. (2013). De novo assembly and characterization of tissue specific transcriptomes in the emerald notothen, Trematomus bernacchii. BMC Genom. *14*, 805–813.
43. Guo, L., Wang, Y., Liang, S., Lin, G., Chen, S., and Yang, G. (2016). Tissue-overlapping response of half-smooth tongue sole (Cynoglossus semilaevis) to thermostressing based on transcriptome profiles. Gene *586*, 97–104.
44. Jesus, T.F., Grosso, A.R., Almeida-Val, V.M.F., and Coelho, M.M. (2016). Transcriptome profiling of two Iberian freshwater fish exposed to thermal stress. J. Therm. Biol. *55*, 54–61.
45. Kim, W.J., Lee, K., Lee, D., Kim, H.C., Nam, B.H., Jung, H., Yi, S.J., and Kim, K. (2021). Transcriptome profiling of olive flounder responses under acute and chronic heat stress. Genes Genomics *43*, 151–159. https://doi.org/10.1007/s13258-021-01053-8.
46. Moore, B., Jolly, J., Izumiyama, M., Kawai, E., Ravasi, T., and Ryu, T. (2024). Tissue-specific transcriptional response of post-larval clownfish to ocean warming. Sci. Total Environ. *908*, 168221.
47. Audzijonyte, A., Richards, S.A., Stuart-Smith, R.D., Pecl, G., Edgar, G.J., Barrett, N.S., Payne, N., and Blanchard, J.L. (2020). Fish body sizes change with temperature but not all species shrink with warming. Nat. Ecol. Evol. *4*, 809–814.
48. Neuheimer, A.B., Thresher, R.E., Lyle, J.M., and Semmens, J.M. (2011). Tolerance limit for fish growth exceeded by warming waters. Nat. Clim. Chang. *1*, 110–113.
49. Moore, B., Jolly, J., Izumiyama, M., Kawai, E., Ryu, T., and Ravasi, T. (2023). Clownfish larvae exhibit faster growth, higher metabolic rates and altered gene expression under future ocean warming. Sci. Total Environ. *873*, 162296.
50. Raventos, N., Torrado, H., Arthur, R., Alcoverro, T., and Macpherson, E. (2021). Temperature reduces fish dispersal as larvae grow faster to their settlement size. J. Anim. Ecol. *90*, 1419–1432.
51. O'Connor, M.I., Bruno, J.F., Gaines, S.D., Halpern, B.S., Lester, S.E., Kinlan, B.P., and Weiss, J.M. (2007). Temperature control of larval dispersal and the implications for marine ecology, evolution, and conservation. Proc. Natl. Acad. Sci. USA *104*, 1266–1271.
52. Fautin, D.G., and Allen, G.R. (1992). Field Guide to Anemonefishes and Their Host Sea Anemones (TFH Publications), pp. 1–65.
53. McMahon, S.J., Parsons, D.M., Donelson, J.M., Pether, S.M.J., and Munday, P.L. (2020). Elevated CO_2 and heatwave conditions affect the aerobic and swimming performance of juvenile Australasian snapper. Mar. Biol. *167*, 6–12.
54. Lefevre, S., Wang, T., and McKenzie, D.J. (2021). The role of mechanistic physiology in investigating impacts of global warming on fishes. J. Exp. Biol. *224*, jeb238840.
55. Volkoff, H., and Rønnestad, I. (2020). Effects of temperature on feeding and digestive processes in fish. Temperature (Austin) *7*, 307–320.
56. Donelson, J.M., Munday, P.L., McCormick, M.I., and Nilsson, G.E. (2011). Acclimation to predicted ocean warming through developmental plasticity in a tropical reef fish. Glob. Change Biol. *17*, 1712–1719.
57. Logan, C.A., and Buckley, B.A. (2015). Transcriptomic responses to environmental temperature in eurythermal and stenothermal fishes. J. Exp. Biol. *218*, 1915–1924. https://doi.org/10.1242/jeb.114397.
58. Zhu, W., Meng, Q., Zhang, H., Wang, M.L., Li, X., Wang, H.T., Zhou, G.L., Miao, L., Qin, Q.L., and Zhang, J.H. (2019). Metabolomics reveals the key role of oxygen metabolism in heat susceptibility of an alpine-dwelling ghost moth, Thitarodes xiaojinensis (Lepidoptera: Hepialidae). Insect Sci. *26*, 695–710.
59. Little, A.G., Loughland, I., and Seebacher, F. (2020). What do warming waters mean for fish physiology and fisheries? J. Fish. Biol. *97*, 328–340.
60. Richards, J.G., Mercado, A.J., Clayton, C.A., Heigenhauser, G.J.F., and Wood, C.M. (2002). Substrate utilization during graded aerobic exercise in rainbow trout. J. Exp. Biol. *205*, 2067–2077.

61. Jia, S., Li, X., Zheng, S., and Wu, G. (2017). Amino acids are major energy substrates for tissues of hybrid striped bass and zebrafish. Amino Acids *49*, 2053–2063.

62. Koukourakis, M.I., Giatromanolaki, A., Polychronidis, A., Simopoulos, C., Gatter, K.C., Harris, A.L., and Sivridis, E. (2006). Endogenous markers of hypoxia/anaerobic metabolism and anemia in primary colorectal cancer. Cancer Sci. *97*, 582–588.

63. Portner, H.O., and Knust, R. (2007). Climate change affects marine fishes through the oxygen limitation of thermal tolerance. Science *315*, 95–97. https://doi.org/10.1126/science.1135471.

64. Rabinowitz, J.D., and Enerbäck, S. (2020). Lactate: the ugly duckling of energy metabolism. Nat. Metab. *2*, 566–571.

65. Hui, S., Ghergurovich, J.M., Morscher, R.J., Jang, C., Teng, X., Lu, W., Esparza, L.A., Reya, T., Zhan, L., Yanxiang Guo, J., et al. (2017). Glucose feeds the TCA cycle via circulating lactate. Nature *551*, 115–118.

66. Campbell, J.E., and Newgard, C.B. (2021). Mechanisms controlling pancreatic islet cell function in insulin secretion. Nat. Rev. Mol. Cell Biol. *22*, 142–158.

67. Stump, C.S., Short, K.R., Bigelow, M.L., Schimke, J.M., and Nair, K.S. (2003). Effect of insulin on human skeletal muscle mitochondrial ATP production, protein synthesis, and mRNA transcripts. Proc. Natl. Acad. Sci. USA *100*, 7996–8001.

68. Polakof, S., Panserat, S., Soengas, J.L., and Moon, T.W. (2012). Glucose metabolism in fish: a review. J. Comp. Physiol. B *182*, 1015–1045.

69. Mirzadeh, Z., Faber, C.L., and Schwartz, M.W. (2022). Central nervous system control of glucose homeostasis: a therapeutic target for type 2 diabetes? Annu. Rev. Pharmacol. Toxicol. *62*, 55–84.

70. Sanz Fernandez, M.V., Stoakes, S.K., Abuajamieh, M., Seibert, J.T., Johnson, J.S., Horst, E.A., Rhoads, R.P., and Baumgard, L.H. (2015). Heat stress increases insulin sensitivity in pigs. Physiol. Rep. *3*, e12478.

71. Wheelock, J.B., Rhoads, R.P., VanBaale, M.J., Sanders, S.R., and Baumgard, L.H. (2010). Effects of heat stress on energetic metabolism in lactating Holstein cows. J. Dairy Sci. *93*, 644–655.

72. Petersen, A.M., and Gleeson, T.T. (2011). Acclimation temperature affects the metabolic response of amphibian skeletal muscle to insulin. Comp. Biochem. Physiol. Mol. Integr. Physiol. *160*, 72–80.

73. Riddle, M.R., Aspiras, A.C., Gaudenz, K., Peuß, R., Sung, J.Y., Martineau, B., Peavey, M., Box, A.C., Tabin, J.A., McGaugh, S., et al. (2018). Insulin resistance in cavefish as an adaptation to a nutrient-limited environment. Nature *555*, 647–651.

74. Sokolova, I.M. (2023). Ectotherm mitochondrial economy and responses to global warming. Acta Physiol. *237*, e13950.

75. Lesnefsky, E.J., and Hoppel, C.L. (2006). Oxidative phosphorylation and aging. Ageing Res. Rev. *5*, 402–433.

76. Acharya, P., Chouhan, K., Weiskirchen, S., and Weiskirchen, R. (2021). Cellular mechanisms of liver fibrosis. Front. Pharmacol. *12*, 671640.

77. Yu, J., Zhong, D., Li, S., Zhang, Z., Mo, H., and Wang, L. (2023). Acute temperature stresses trigger liver transcriptome and microbial community remodeling in largemouth bass (Micropterus salmoides). Aquaculture *573*, 739573.

78. Han, P., Qiao, Y., He, J., and Wang, X. (2023). Stress responses to warming in Japanese flounder (Paralichthys olivaceus) from different environmental scenarios. Sci. Total Environ. *897*, 165341.

79. Jia, G., Feng, J., and Qin, Z. (2006). Studies on the fatty liver diseases of Sciaenops ocellatus caused by different ether extract levels in diets. Front. Biol. China *1*, 9–12.

80. Schneider, V.A., and Granato, M. (2006). The myotomal diwanka (lh3) glycosyltransferase and type XVIII collagen are critical for motor growth cone migration. Neuron *50*, 683–695.

81. Fox, M.A., Sanes, J.R., Borza, D.-B., Eswarakumar, V.P., Fässler, R., Hudson, B.G., John, S.W.M., Ninomiya, Y., Pedchenko, V., Pfaff, S.L., et al. (2007). Distinct target-derived signals organize formation, maturation, and maintenance of motor nerve terminals. Cell *129*, 179–193.

82. Huizinga, J.D., and Lammers, W.J.E.P. (2009). Gut peristalsis is governed by a multitude of cooperating mechanisms. Am. J. Physiol. Gastrointest. Liver Physiol. *296*, G1–G8.

83. Gräns, A., Seth, H., Axelsson, M., Sandblom, E., Albertsson, F., Wiklander, K., and Olsson, C. (2013). Effects of acute temperature changes on gut physiology in two species of sculpin from the west coast of Greenland. Polar Biol. *36*, 775–785.

84. Burka, J.F., Briand, H.A., Purcell, L.M., and Ireland, W.P. (1993). The effects of acute temperature change on smooth muscle contractility of rainbow trout (Oncorhynchus mykiss Walbaum) intestine. Fish Physiol. Biochem. *12*, 53–60.

85. König, J., Wells, J., Cani, P.D., García-Ródenas, C.L., MacDonald, T., Mercenier, A., Whyte, J., Troost, F., and Brummer, R.-J. (2016). Human intestinal barrier function in health and disease. Clin. Transl. Gastroenterol. *7*, e196.

86. Stosik, M., Tokarz-Deptuła, B., and Deptuła, W. (2023). Immunity of the intestinal mucosa in teleost fish. Fish Shellfish Immunol. *133*, 108572.

87. Zimmer, A.M., and Perry, S.F. (2022). Physiology and aquaculture: A review of ion and acid-base regulation by the gills of fishes. Fish Fish. *23*, 874–898.

88. Evans, D.H., Piermarini, P.M., and Choe, K.P. (2005). The multifunctional fish gill: dominant site of gas exchange, osmoregulation, acid-base regulation, and excretion of nitrogenous waste. Physiol. Rev. *85*, 97–177.

89. Yang, S., Li, D., Feng, L., Zhang, C., Xi, D., Liu, H., Yan, C., Xu, Z., Zhang, Y., Li, Y., et al. (2023). Transcriptome analysis reveals the high temperature induced damage is a significant factor affecting the osmotic function of gill tissue in Siberian sturgeon (Acipenser baerii). BMC Genom. *24*, 2.

90. Masroor, W., Farcy, E., Blondeau-Bidet, E., Venn, A., Tambutté, E., and Lorin-Nebel, C. (2019). Effect of salinity and temperature on the expression of genes involved in branchial ion transport processes in European sea bass. J. Therm. Biol. *85*, 102422.

91. Bolger, A.M., Lohse, M., and Usadel, B. (2014). Trimmomatic: a flexible trimmer for Illumina sequence data. Bioinformatics *30*, 2114–2120.

92. Kim, D., Paggi, J.M., Park, C., Bennett, C., and Salzberg, S.L. (2019). Graph-based genome alignment and genotyping with HISAT2 and HISAT-genotype. Nat. Biotechnol. *37*, 907–915.

93. Li, H., Handsaker, B., Wysoker, A., Fennell, T., Ruan, J., Homer, N., Marth, G., Abecasis, G., and Durbin, R.; 1000 Genome Project Data Processing Subgroup (2009). The sequence alignment/map format and SAMtools. Bioinformatics *25*, 2078–2079.

94. Pertea, M., Kim, D., Pertea, G.M., Leek, J.T., and Salzberg, S.L. (2016). Transcript-level expression analysis of RNA-seq experiments with HISAT, StringTie and Ballgown. Nat. Protoc. *11*, 1650–1667.

95. Love, M.I., Huber, W., and Anders, S. (2014). Moderated estimation of fold change and dispersion for RNA-seq data with DESeq2. Genome Biol. *15*, 550.

96. Yu, G., Wang, L.-G., Han, Y., and He, Q.-Y. (2012). clusterProfiler: an R package for comparing biological themes among gene clusters. OMICS A J. Integr. Biol. *16*, 284–287.

97. Harbig, T., Paz, M.W., and Nieselt, K. (2023). GO-Compass: Visual Navigation of Multiple Lists of GO terms. Computer Graphics Forum *42*, 271–281.

98. Kolde, R., and Kolde, M.R. (2015). Package 'pheatmap'. R package 1, 790.

99. IPCC (2021). IPCC, 2021: Summary for Policymakers. In Climate Change 2021: The Physical Science Basis. Contribution of Working Group I to the Sixth Assessment Report of the Intergovernmental Panel on Climate Change, V. MassonDelmotte, P. Zhai, A. Pirani, S.L. Connors, C. Péan, S. Berger, N. Caud, Y. Chen, L. Goldfarb, and M.I. Gomis, et al., eds. (Cambridge University Press), pp. 3–32. https://doi.org/10.1017/9781009157896.001.

100. Hobday, A.J., Alexander, L.V., Perkins, S.E., Smale, D.A., Straub, S.C., Oliver, E.C.J., Benthuysen, J.A., Burrows, M.T., Donat, M.G., Feng, M., et al. (2016). A hierarchical approach to defining marine heatwaves. Prog. Oceanogr. *141*, 227–238.

101. Roux, N., Logeux, V., Trouillard, N., Pillot, R., Magré, K., Salis, P., Lecchini, D., Besseau, L., Laudet, V., and Romans, P. (2021). A star is born again: Methods for larval rearing of an emerging model organism, the False clownfish Amphiprion ocellaris. J. Exp. Zool. B Mol. Dev. Evol. *336*, 376–385.

102. Svendsen, M.B.S., Bushnell, P.G., and Steffensen, J.F. (2016). Design and setup of intermittent-flow respirometry system for aquatic organisms. J. Fish. Biol. *88*, 26–50.

103. Clark, T.D., Sandblom, E., and Jutfelt, F. (2013). Aerobic scope measurements of fishes in an era of climate change: respirometry, relevance and recommendations. J. Exp. Biol. *216*, 2771–2782. https://doi.org/10.1242/jeb.084251.

104. Chabot, D., Steffensen, J.F., and Farrell, A.P. (2016). The determination of standard metabolic rate in fishes. J. Fish. Biol. *88*, 81–121.

105. Donelson, J.M., Munday, P.L., McCormick, M.I., and Pitcher, C.R. (2012). Rapid transgenerational acclimation of a tropical reef fish to climate change. Nat. Clim. Chang. *2*, 30–32. https://doi.org/10.1038/nclimate1323.

106. Ryu, T., Herrera, M., Moore, B., Izumiyama, M., Kawai, E., Laudet, V., and Ravasi, T. (2022). A chromosome-scale genome assembly of the false clownfish. G3 (Bethesda). *12*, jkac074. https://doi.org/10.1093/g3journal/jkac074.

107. Gene Ontology Consortium (2004). The Gene Ontology (GO) database and informatics resource. Nucleic Acids Res. *32*, D258–D261.

108. Imai, J., Katagiri, H., Yamada, T., Ishigaki, Y., Suzuki, T., Kudo, H., Uno, K., Hasegawa, Y., Gao, J., Kaneko, K., et al. (2008). Regulation of pancreatic β cell mass by neuronal signals from the liver. Science *322*, 1250–1254.

109. Rodriguez-Diaz, R., Menegaz, D., and Caicedo, A. (2014). Neurotransmitters act as paracrine signals to regulate insulin secretion from the human pancreatic islet. J. Physiol. *592*, 3413–3417.

110. Dolai, S., Xie, L., Zhu, D., Liang, T., Qin, T., Xie, H., Kang, Y., Chapman, E. R., and Gaisano, H.Y. (2016). Synaptotagmin-7 functions to replenish insulin granules for exocytosis in human islet β-cells. Diabetes *65*, 1962–1976.

111. Wang, L., Sui, L., Panigrahi, S.K., Meece, K., Xin, Y., Kim, J., Gromada, J., Doege, C.A., Wardlaw, S.L., Egli, D., and Leibel, R.L. (2017). PC1/3 deficiency impacts pro-opiomelanocortin processing in human embryonic stem cell-derived hypothalamic neurons. Stem Cell Rep. *8*, 264–277.

112. Suckow, A.T., Comoletti, D., Waldrop, M.A., Mosedale, M., Egodage, S., Taylor, P., and Chessler, S.D. (2008). Expression of neurexin, neuroligin, and their cytoplasmic binding partners in the pancreatic β-cells and the involvement of neuroligin in insulin secretion. Endocrinology *149*, 6006–6017.

STAR★METHODS

KEY RESOURCES TABLE

REAGENT or RESOURCE	SOURCE	IDENTIFIER
Chemicals, peptides, and recombinant proteins		
RNA Later	Sigma-Aldrich, St. Louis, USA	R0901
Maxwell® RSC simplyRNA Tissue Kit	Promega, Madison, USA	AS1340
TruSeq stranded mRNA Sample Preparation Kit	Illumina, CA, USA	20020594
Deposited data		
RNA-Sequencing Data	NCBI – This Paper	PRJNA1094601
Experimental models: Organisms/strains		
Amphiprion ocellaris	Okinawa Institute of Science and Technology Marine Station – This Paper	N/A
Software and algorithms		
Loligo Systems AutoResp	Loligo Systems, Toldboden, Denmark	https://www.loligosystems.com/products/respirometry/software/autoresp-v3-software-for-automated-intermittent-respirometry/
Trimmomatic v0.39	Bolger et al.[91]	http://www.usadellab.org/cms/?page=trimmomatic
HISAT2 v2.2.1	Kim et al.[92]	https://daehwankimlab.github.io/hisat2/
SAMtools v1.10	Li et al.[93]	https://www.htslib.org/
StringTie v2.1.4	Pertea et al.[94]	https://ccb.jhu.edu/software/stringtie/
DESeq2 v1.26.0	Love et al.[95]	https://bioconductor.org/packages/release/bioc/html/DESeq2.html
ClusterProfiler	Yu et al.[96]	https://bioconductor.org/packages/release/bioc/html/clusterProfiler.html
GO-Compass	Harbig et al.[97]	https://go-compass-tuevis.cs.uni-tuebingen.de/
pheatmap v1.0.12	Kolde et al.[98]	https://www.rdocumentation.org/packages/pheatmap/versions/1.0.13/topics/pheatmap
R v3.6.1	R Foundation	https://www.r-project.org/
Other		
Loligo Systems Respirometry System	Loligo Systems, Toldboden, Denmark	https://www.loligosystems.com/products/respirometry/systems/core-resting-respirometry-system-4-chhid9l20230v50hz/

EXPERIMENTAL MODEL AND STUDY PARTICIPANT DETAILS

All *A. ocellaris* were sourced from breeding pairs collected from around Okinawa and housed at Okinawa Institute of Science and Technology Marine Science Station (Table S37). With a flow-through system supplied from ocean intake pipes, parental tank temperatures follow the natural seasonal cycle of Okinawa. Following spawning, eggs remained in parental tanks during embryonic development, with parental tank inflow water having a mean temperature of 29.01 °C across the two-week period that encompassed the fertilisation-hatching of all clutches. The evening prior to hatching eggs were transferred to larval rearing tanks in a 5 L beaker. Here, a handheld thermometer (Fisherbrand, Traceable) was used to ensure water within the beaker was at 28 ± 0.5 °C before eggs were place into 28 °C, in 35 L larval tanks. Within larval tanks temperature was regulated by a REI-SEA thermo-controller (TC-101) and two 150 W (Kotobuki) heaters, with air stones used to maintain oxygen levels. All animals and protocols utilised in this study were approved by Okinawa Institute of Science and Technology Animal Care and Use Committee.

METHOD DETAILS

Experimental design

A. ocellaris were exposed to three different experimental treatments, denoted as 28 °C constant (T28), 31 °C constant (T31), and 31 °C Early-life Thermal Stress (ETS) immediately after hatching (Figure 1). The 28 °C constant treatment (T28) was designated as

the control, as this is the average temperature of Okinawan oceans in summer (mean temperature of 27.71 °C in July-September 2021; Okinawa Institute of Science and Technology, unpublished data), and thus fish in this treatment were exposed to 28 °C from 1 to 60 days post hatch (dph). The 31 °C constant treatment (T31) was designed to simulate summer temperatures in Okinawa under future ocean warming, based on IPCC SSP3 - 7.0 predictions,[99] and thus fish in this treatment were exposed to 31 °C from 1 to 60 dph. The 31 °C Early-life thermal stress treatment (ETS) was designed to reflect future marine heatwaves,[2,100] in which fish could be exposed to temperatures beyond their natural thermal limits for a short period of time. Therefore, fish in this treatment were exposed to 31 °C from 1 to 20 dph (entire larval development period) and 28 °C from 21 to 60 dph. Such an approach allows for the lasting effects of early-life thermal stress, and potential developmental programming to be investigated. At the end of these initial treatments, juvenile *A. ocellaris* were subjected to metabolic trials (at 59 dph) and sampled for RNA-Seq (at 60 dph) at their current treatment temperature, being either 28 °C (S28) or 31 °C (S31). Following sampling at 59 and 60 dph, temperatures within each treatment were reversed, so that temperatures in T28 and ETS were raised to 31 °C and temperatures in T31 were reduced to 28 °C. These 3 °C changes in temperature were achieved by increasing/reducing the temperature by 0.5 °C/h. Juveniles were then subjected to metabolic trials at 61 dph. Furthermore, fish that experienced acute warming from the temperature reversal (S31) were sampled for RNA-Seq (at 62 dph). This approach allowed the effects of acute temperature stress (1–2 days) to be investigated, whilst also providing information on how thermal history impacts this response. These three experimental treatments and two sampling temperatures per treatment, resulted in a total of six experimental groups, assigned the IDs: T28.S28, T28.S31, T31.S31, T31.S28, ETS.S28, ETS.S31 (Figure 1).

Larval-juvenile rearing

The morning following hatching (one dph) larvae from the same clutch were split evenly between 28 °C and 31 °C rearing tanks, with temperature raised by 0.5 °C every 2 h to the 31 °C target. During the larval rearing period T31 and ETS fish were raised together, as both required a temperature of 31 °C for the first 20 days. Therefore, each clutch was split evenly between two separate larval rearing tanks. A total of three clutches of eggs, coming from three different breeding pairs (genotypes) were used to ensure genetic diversity within the study, giving a total of six larval rearing tanks. Due to the number of eggs differing between clutches, variable larval mortality through time, and the fragility of one dph larvae, the exact number of larvae per tank was unknown. However, visual observation was used to ensure larvae from each clutch were split as evenly as possible between the 28 °C and 31 °C treatments, with final larval numbers at 20 dph not differing by > 16 across all tanks. Larvae were reared following same protocols as in Moore et al.,[49] following the best practices detailed in Roux et al.[101]

At 20 dph, 24 individuals from each clutch were selected at random and transferred to the OIST Marine Heatwave Simulator Aquaria System in a 1 L beaker containing larval tank water. Here, two fish were placed in each 40 L experimental tank, separated by plastic mesh dividers with temperature maintained at either 28 °C or 31 °C. Mesh dividers separated individuals physically, however interactions between fish were still possible. T28 and T31 fish were placed in the same temperatures they were reared in as larvae, whereas fish in the ETS treatment were transferred to 31 °C tanks, before the temperature was then reduced to 28 °C across a 12h period. This approach gave a total of 24 fish per treatment (eight per clutch). Juvenile *A. ocellaris* were raised in this system from 21 to 62 dph and fed a mix of Otohime B2 and Otohime C2 marine larval grow out feed twice per day, with tanks cleaned and siphoned daily to remove waste and prevent algal build-up. See Table S38 for information on experimental treatment temperatures from 2 to 20 dph.

Physiological measurements

Metabolic trials were conducted using a Loligo Systems 8-chamber (240 mL) Resting Respirometry System and the associated Loligo Systems AutoResp software. Here, individual metabolic chambers were placed within 40 L tanks of the OIST Marine Heatwave Simulator Aquaria System, that were used to regulate temperature at either 28 °C or 31 °C. Prior to metabolic measurements fish were not fed for 24 h[102,103] and wet-weight of the fish was measured. Intermittent respirometry was utilized with all measurements following a 5-min measurement, 30 s flush, 40 s wait protocol. Metabolic rates were calculated from oxygen concentration change in each 5-min measurement period, using the equation $MO_2 = K^*V^*\beta/M$, where K is the rate of oxygen decline over time, V is the respirometer volume, β is the solubility of oxygen in water, and M is the fish body mass. Prior to each trial starting, background respiration in each chamber was measured by placing them in darkness and recording oxygen concentration for 15 min, with the same measurement of background respiration conducted at the end of each trial. When fish were added to each chamber with a handheld net a 3-h metabolic rate trial began, with the first 2 h representing an acclimation period. Here, a 2-h acclimation was utilized as the young age (60 dph) and acute temperature treatments tested, resulted in a small window in which measurements could take place, therefore longer acclimation periods such as those recommended in[104] could not be utilized. However, inspection of MO_2 values indicated they plateaued within this period, and previous studies of related species have adopted similar reduced trial periods.[53,105] RMR was then determined by taking the mean of the lowest 10 (low10) MO_2 values recorded in the final hour (described in Chabot et al.). Although the use of reduced acclimation periods and the low10 protocol have previously been utilised to measure standard metabolic rate in fish, here we refer to RMR as minor pectoral fin activity was observed for fish within the chambers. Final RMR was calculated by subtracting mean background respiration and normalizing by the wet-weight of fish to give an RMR unit of mg O_2 kg^{-1} h^{-1}.

At 59 and 61 dph, 14–15 juveniles (4–5 per genotype) were tested per treatment giving a total of 43–44 RMR trials per timepoint. As nine individuals were sampled for RNA-Seq (see below) on 60 dph, only 15 individuals remained per treatment, and thus 5–6 of the 14–15 individuals subjected to RMR measurements at 62 dph had undergone metabolic testing at 59 dph. However, the number of individuals tested twice was kept consistent between treatments and clutches. Prior to metabolic measurements all fish were weighed, and wet-weight was recorded. The two weight measurements of individuals subjected to repeat metabolic testing were averaged for later analysis, to ensure a single treatment-level weight for each fish was obtained.

RNA sequencing sampling

At 60 dph, nine fish per treatment (three per genotype) were randomly selected for dissection and tissue extraction, with all nine undergoing metabolic trials the day prior. Of these nine, six were subjected to RNA-Seq (two per genotype). No individual subjected to RNA-Seq underwent metabolic testing twice. This process was repeated at 62 dph at the reverse sampling temperatures, however fish in T31.S28 group were not subjected to RNA-Seq (Figure 1). This decision was taken as it was deemed that gene expression profiles of individuals raised at 31 °C for 60 days, before being exposed to control temperatures of 28 °C for two days, provided limited ecologically relevant information. All fish subjected to RNA-Seq were fed the evening before sampling (18:00), following metabolic trials. Following collection from the tank, fish were euthanized by severing the spinal cord and transferred to a Petri dish for dissection. Dissections were carried out under an Olympus SZ61 stereomicroscope (Olympus Corporation, Tokyo, Japan), with the brain, gill, heart, intestine, liver, muscle, and pancreas of each individual extracted. Tissues were immediately placed in RNAlater (Sigma-Aldrich, St. Louis, USA) and stored at −20 °C. A total of 45 fish underwent dissection and tissue extraction across the two sampling timepoints, with six biological replicates (n = 6) for each of the tissue/treatment/sampling temperature combinations sequenced (30 fish total).

Nucleic acid extraction and sequencing

Total RNA was extracted from 210 tissues (30 fish x 7 tissues) using a Maxwell RSC simplyRNA Tissue Kit (Promega, Madison, USA) and the associated Maxwell RSC Instrument (Promega, Madison, USA), following the manufacturers guidelines. The quality and quantity of extracted total RNA was assessed using an Invitrogen QuBit Flex Fluorometer (Invitrogen, Waltham, USA) and an Agilent TapeStation 4200 (Agilent Technologies, Santa Clara, USA). RNA quality control, library preparation, and sequencing was conducted by Theragen Bio (Seongnam, Korea) (Table S39). Here, RNA libraries were prepared from total RNA using a TruSeq stranded mRNA Sample Preparation Kit (Illumina, CA, USA). Following library preparation, 151 bp paired end mRNA sequencing was conducted on an Illumina NovaSeq 6000 platform (Illumina, CA, USA).

QUANTIFICATION AND STATISTICAL ANALYSIS

Physiology: Statistical analyses

The effect of treatment and sampling temperature on juvenile RMR was assessed using a linear mixed effects model with treatment, sampling temperature and weight, as fixed factors and genotype and tank as nested random factors. Additionally, the effect of treatment on juvenile wet-weights was investigated using a linear mixed effects model with treatment as a fixed factor and genotype and tank as nested random factors. F-tests were used to compare variances amongst fixed and random factors. Differences between experimental groups were assessed using least-square means (lsmeans) multiple comparisons post hoc tests (with Tukey's correction). For wet-weight, sampling temperature was ignored as it was deemed that ∼1 day exposure to the reverse temperature would not influence wet-weight. Assumptions of all models were checked via visual inspection of residuals and standard model diagnostic tests were conducted using DHARMa v0.4.4. All analyses were performed in R version 3.6.1.

RNA-sequencing: Bioinformatic analysis

Following RNA-Seq, the number of reads per sample ranged from 40,000,000 to 180,000,000 (Table S40). Reads were trimmed with Trimmomatic v0.39[91] and the parameters: "TruSeq3-PE.fa:2:30:10:8: keepBothReads LEADING:3 TRAILING:3 MINLEN:36.". Trimmed reads were mapped to a chromosome-scale *A. ocellaris* genome[106] using HISAT2 v2.2.1,[92] and resulting SAM files were converted to BAM files using SAMtools v1.10.[93] BAM files and the associated *A. ocellaris* gene annotation[106] were used as input for StringTie v2.1.4 to quantify expression levels.[94] Gene-specific raw reads counts were generated from the StringTie output using the python script prepDE.py3.[94] and differential gene expression between experimental groups was quantified using DESeq2 v1.26.0.[95] A total of 26,642 genes were expressed, with filtering for genes with counts <10 across samples giving a total of 26,244 genes subjected to further analyses. Here, as the aim was conduct specific pairwise comparisons rather than test fixed/interactive effects, experimental factors (treatment, sampling temperature, tissue) were combined into a single factor (design: ∼combinedfactor) as recommended in the DESeq2 vignette.[95] Pairwise comparisons (contrasts) between T31.S31 and T28.S28 (T31.S31vT28.S28), T28.S31 and T28.S28 (T28.S31vT28.S28), ETS.S31 and ETS.S28 (ETS.S31vETS.S28), and ETS.S28 and T28.S28 (ETS.S28vT28.S28) were assessed for each tissue. Contrasts between these experimental groups were selected as the aim was to investigate; 1) the chronic effect of 31 °C (T31.S31vT28.S28), 2) the acute effect of 31 °C (T28.S31vT28.S28), 3) the acute effect of 31 °C following early-life stage exposure to elevated temperatures (ETS.S31vETS.S28), and 4) the lasting effects of early-life

thermal stress (ETS.S28vT28.S28). Within these pairwise comparisons genes with an adjusted p-value <0.05 (corrected by Benjamini-Hochberg (BH) method) and an abs(log_2FoldChange) > one were identified as DEGs.

Following gene expression analysis, the "enricher" function of the ClusterProfiler package[96] and Gene Ontology (GO) terms,[107] including the molecular function and biological process categories were used to perform functional enrichment analysis on groups of DEGs. The number of common GO terms between contrasts for each tissue was investigated with GO-Compass,[97] with a correlation heatmap used to visualize Pearson's correlation of the GO term p-values.[97] Additionally, functional enrichment analysis of groups of DEGs was also conducted with Kyoto Encyclopedia of Genes and Genomes (KEGG) pathways, with Kegg Orthology (KO) terms and the *enricher* clusterprofiler function[96] used to identify enriched KEGG pathways in each contrast. Functional enrichment analysis of GO and KEGG terms were corrected for multiple testing using the BH approach. As multiple GO terms and KEGG pathways related to "insulin" were enriched in the pancreas, genes involved in insulin synthesis and secretion were further investigated. DEGs associated with enriched GO terms (present in $\geq$ one contrast) related to insulin synthesis/secretion or neural signaling were extracted. Neural signaling GO terms were utilized for insulin signaling analysis as neuronal signaling is known to underpin tissue-to-tissue cross talk between the pancreas and other tissues involved in metabolism,[108] whilst many signaling pathways involved in insulin synthesis/release are similar to those involved in neural signaling.[109] For example, synaptotagmin-7 (*syt-7*) is a component of exocytotic machinery in neurons, but also mediates glucose-stimulated insulin secretion in pancreatic cells of rodents,[110] neuroendocrine convertase 1 (*pcsk1*) is responsible for processing prohormones and neuropeptides in neuroendocrine tissues,[111] and neuroligins are involved in the formation of glutamatergic/GABAergic synapses, as well as insulin secretion in INS-1 β-cells and rat islet cells.[112] Moreover, the voltage-dependent calcium channel *cacna1d*, the ATP-binding cassette *abcc8*, and the calcium-activated potassium channel (*kcnn3*) are all listed within the "insulin secretion" KEGG pathway (KO04911), however these genes are only present in neural signaling related GO terms, and not in the "insulin secretion" GO term.

Following identification of insulin-related DEGs, these genes were mapped to the "insulin secretion" KEGG pathway, and for visual representation of expression, DESeq2 normalized gene counts were extracted, averaged for each treatment and sampling temperature group, plus one added, and log_2 transformed. Similarly, as multiple genes within the "oxidative phosphorylation" KEGG pathway (KO00190) were upregulated in the T31.S31vT28.S28 contrast, expression levels of these genes were visualized across experimental groups using the pheatmap v1.0.12 package.[98] Finally, genes involved in glucose uptake and metabolism were identified from DEGs from all contrasts of all tissue types.